13. T.-C. He *et al.*, *Proc. Natl. Acad. Sci. U.S.A.* **95**, 2509 (1998).
14. W. Bains, P. Ponte, H. M. Blau, L. Kedes, *Mol. Cell. Biol.* **4**, 1449 (1984).
15. T. Centner *et al.*, *J. Mol. Biol.* **306**, 717 (2001).
16. P. S. Freemont, *Curr. Biol.* **10**, R84 (2000).
17. C. A. Joaeiro, A. M. Wiessman, *Cell* **102**, 549 (2000).
18. D. B. Thomason, R. E. Herrick, D. Surdyka, K. M. Baldwin, *J. Appl. Physiol.* **63**, 130 (1987).
19. A. Chen *et al.*, *J. Biol. Chem.* **275**, 15432 (2000).
20. We thank L. S. Schleifer and P. R. Vagelos for their enthusiastic support; E. Burrows, B. Efraim, and V. Lan for expert graphics work; and M. Gonzalez for insightful discussions. We thank members of the Muscle in vivo and in vitro groups, transgenic group, and tissue culture group for their expert technical assistance.

30 August 2001; accepted 17 October 2001
Published online 25 October 2001;
10.1126/science.1065874
Include this information when citing this paper.

Taking Cell-Matrix Adhesions to the Third Dimension

Edna Cukierman, Roumen Pankov, Daron R. Stevens, Kenneth M. Yamada*

Adhesions between fibroblastic cells and extracellular matrix have been studied extensively in vitro, but little is known about their in vivo counterparts. Here, we characterized the composition and function of adhesions in three-dimensional (3D) matrices derived from tissues or cell culture. "3D-matrix adhesions" differ from focal and fibrillar adhesions characterized on 2D substrates in their content of $\alpha_5\beta_1$ and $\alpha_v\beta_3$ integrins, paxillin, other cytoskeletal components, and tyrosine phosphorylation of focal adhesion kinase (FAK). Relative to 2D substrates, 3D-matrix interactions also display enhanced cell biological activities and narrowed integrin usage. These distinctive in vivo 3D-matrix adhesions differ in structure, localization, and function from classically described in vitro adhesions, and as such they may be more biologically relevant to living organisms.

Our current understanding of cell-matrix adhesions—the cell surface structures that mediate cell interactions with extracellular matrix (ECM)—is based primarily on in vitro studies of focal adhesions and other adhesive structures, particularly in fibroblasts (*1*–*4*). Focal adhesions are integrin-based structures that mediate strong cell-substrate adhesion and transmit information in a bidirectional manner between extracellular molecules and the cytoplasm (*1*–*7*). A second structure termed the fibrillar adhesion (*8*) functions in generating extracellular fibrils of fibronectin (*9*). Our knowledge about the roles of these structures in cell adhesion, migration, signaling, and cytoskeletal function is derived primarily from studies on planar 2D tissue culture substrates. However, the importance of 3D ECM is recognized for epithelial cells, where 3D environments promote normal epithelial polarity and differentiation (*10*). Fibroblastic cells have been studied mainly in 2D cell cultures, yet culturing them on flat substrates induces an artificial polarity between the lower and upper surfaces of these normally nonpolar cells; not surprisingly, fibroblast morphology and migration differ once suspended in collagen gels (*11*, *12*). Relatively little is known about the cell-matrix adhesive structures formed in 3D matrices of living tissues, particularly in the natural in vivo environments of migrating cells during embryonic development.

Using current knowledge about the molecular composition and functions of the in vitro cell-matrix adhesions formed by fibroblasts, we searched for comparable structures in 3D environments. In 2D cell culture, focal and fibrillar adhesions have distinct molecular compositions: Focal ad-

Craniofacial Developmental Biology and Regeneration Branch, National Institute of Dental and Craniofacial Research, National Institutes of Health, Bethesda, MD 20892, USA.

*To whom correspondence should be addressed. E-mail: ky4w@nih.gov

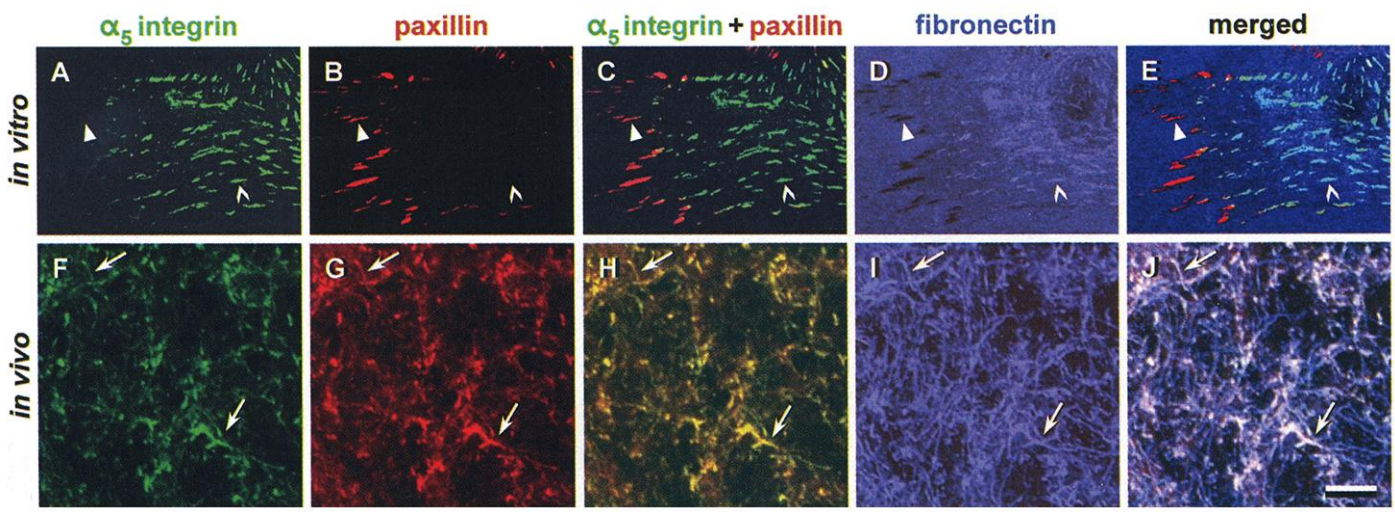

Fig. 1. In vivo 3D-matrix adhesions differ from focal or fibrillar adhesions on 2D substrates. (**A** to **E**) Confocal images of indirect immunofluorescence staining of an NIH-3T3 mouse fibroblast in vitro on a 2D fibronectin-coated cover slip; (**F** to **J**) transverse cryostat craniofacial mesenchyme sections of an E13.5 mouse embryo. α_5 integrin [(A) and (F), green] and paxillin [(B) and (G), red] colocalize in a fibrillar organization in mesenchymal tissue [(H), yellow in merged image indicates overlap of red and green labels], but not on a 2D substrate in vitro (C). Fibronectin [(D) and (I), blue] localizes to fibrillar structures in vivo, and merged images indicate substantial overlap of all three molecules [(J), white compared to (E)]. Note that focal adhesions (filled arrowheads) and fibrillar adhesions (open arrowheads) show differential localization of the α_5 integrin and paxillin markers only on traditional flat 2D substrates in vitro. The 3D-matrix adhesions (arrows) identified by triple localization are present in 3D environments in vivo. Scale bar, 5 μm.

hesions characteristically contain integrin $\alpha_v\beta_3$ as well as plaque proteins such as paxillin, vinculin, and FAK, whereas fibrillar adhesions are composed prominently of $\alpha_5\beta_1$ integrin and tensin (*8*). Molecules such as FAK (*13*) and paxillin (*14*) serve as markers for focal adhesions. In three dimensions, we found that paxillin and α_5 integrin colocalized to unusual cell-matrix attachments parallel to fibronectin-containing extracellular fibers (Fig. 1, F to J) (*15*) rather than localizing separately to classical focal and fibrillar adhesions, respectively. These molecules were co-organized in distinctive structures on mesenchymal and migrating mouse neural crest cells, for which we propose the term "3D-matrix adhesions."

To determine whether 3D-matrix adhesions were associated with different physiological responses of cells (*16*) compared to those mediated by classical adhesions to planar surfaces, we plated human foreskin fibroblasts onto cell-free 3D matrices derived either from detergent-extracted mouse embryo sections ("tissue-derived 3D matrices") or from naturally deposited 3D ECMs of NIH-3T3 fibroblasts that were denuded of cells ("cell-derived 3D matrices") (*17*). As controls, human fibroblasts were also plated onto simple 2D ECM substrates of fibronectin, laminin, or collagen I, as well as 3D collagen gel lattices (Fig. 2), or onto 2D coatings of solubilized, cell-derived 3D matrices at various concentrations (2D mix) or 3D matrices that were mechanically compressed (2D matrix) (*17*).

The cell-derived 3D matrix was more effective (by a factor of >6) in mediating cell adhesion than were 2D substrates or 3D collagen gels, as quantified by a 10-min cell attachment assay (Table 1 and Fig. 2A) (*18*). A similar enhancement (by a factor of 5) of attachment to tissue-derived 3D matrix was also observed (*19*). Cells also showed enhanced migration rates (by a factor of ~1.5) in 3D matrices relative to individual protein-coated surfaces (Table 1 and Fig. 2C) and an accelerated rate of acquisition of a characteristic in vivo–like spindle-shaped morphology (Table 1 and Fig. 2B). Although the overall cell shapes were eventually similar for cells in collagen I gels after 18 hours [compare (*11*)], cells in 3D matrices had fewer branched terminal processes, and morphological asymmetry was achieved at earlier time points. More-

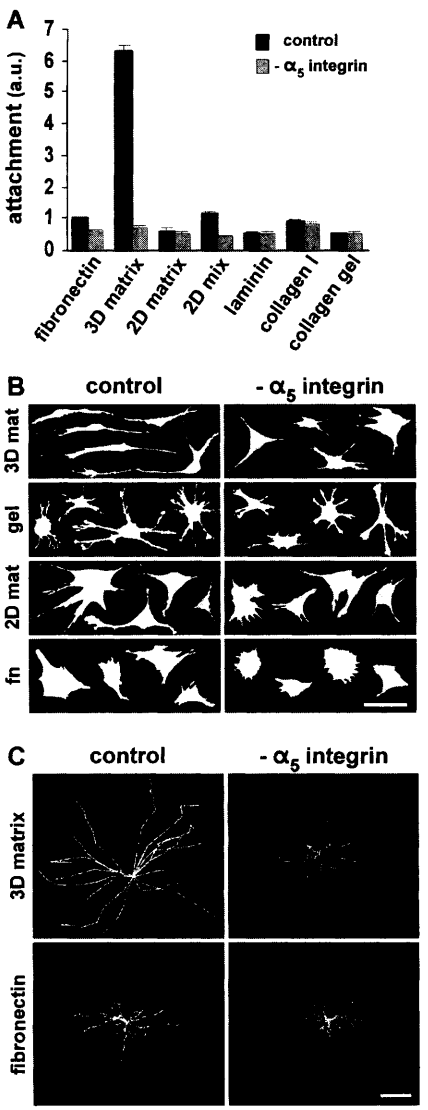

Fig. 2. Enhancement of cellular responses and α_5 integrin dependence in cell-derived 3D matrices. Four different functional responses were tested for human foreskin fibroblasts plated onto cell-derived 3D matrix in comparison to 2D surfaces coated with each of the purified ECM proteins fibronectin, laminin-1, or collagen I; 2D coating with solubilized (2D mix) or mechanically compressed cell-derived matrix (2D matrix); or 3D collagen gel lattices. For quantitative analyses, see (*18*). (**A**) Fibroblast attachment to the indicated substrates. Black and gray columns indicate untreated control or treatment with function-blocking α_5 integrin mAb16 (– α_5 integrin), respectively. Arbitrary units (a.u.) denote relative numbers of cells attached to fibronectin 10 min after plating; error bars are SEM. (**B**) Typical morphologies of cells on different substrates. Human fibroblasts were stained with DiI for visualization (*16*). Each vertical set of four panels shows thresholded digital images of four representative cells with a mean EFF equivalent to the mean of each total sample of 18 to 50 cells. Fibroblasts were plated on cell-derived 3D matrix (3D mat), 3D collagen lattices (gel), mechanically flattened cell-derived matrix (2D mat), or fibronectin-coated surface (fn) in the presence of mAb16 (– α_5 integrin) or in its absence (control) for 5 hours. Note that fibroblasts in 3D matrix achieved their final, elongated morphology by 5 hours (3D mat, control). Although fibroblasts on cell-derived 2D matrices eventually achieved the same morphology after 18 hours, only the morphology of cells in cell-derived 3D matrices was affected by the presence of the function-blocking α_5 integrin mAb (*19*). (**C**) Human fibroblast migration traced by time-lapse video microscopy (*26*). Sixteen representative paths for each treatment were positioned with a common origin to generate a starlike pattern; faster migration produced larger stars. The motility of cells was recorded on the indicated substrates for 8 hours in the presence (– α_5 integrin) or absence (control) of mAb16. Scale bars, 100 μm.

Table 1. Cell biological responses and effects of inhibiting the α_5 integrin (*16–18*). RS, relative stimulation versus fibronectin; α_5I, α_5 inhibition expressed as a percentage relative to the untreated control on the same substrate. Assay data are expressed as follows. Attachment assay: Arbitrary units (a.u.) denote relative numbers of attached cells compared to fibronectin 10 min after plating. Cell morphologyassay: EFF = elliptical form factor (length/breadth) at 5 or 18 hours. Movement assay: mean velocity determined by time-lapse recording. Proliferation assay: % BrdU = [BrdU-positive cells (proliferative)]/[lamin B–positive cells (total)] × 100. *$P < 0.05$, **$P < 0.01$, ***$P < 0.001$; statistical analyses were by analysis of variance or by Kruskal-Wallis tests for the attachment assays.

Assay	Fibronectin		3D matrix		2D matrix		2D mix		Laminin		Collagen I		Collagen gel	
	RS	α_5I (%)	RS	α_5I (%)	RS	α_5I (%)	RS	α_5I (%)	RS	α_5I (%)	RS	α_5I (%)	RS	α_5I (%)
Attachment (a.u.)	1.0	36***	6.3***	88***	0.6***	13	1.1	62***	0.5***	3	0.9	7	0.5***	−2
Cell morphology														
(EFF, 5 hours)	1.0	29*	2.9***	68***	0.9	13	1.0	32	0.9	2	0.8	−17	0.9	−9
(EFF, 18 hours)	1.0	34*	1.9***	56***	1.9***	7	1.6**	8	1.1	3	1.3	18	1.2	−11
Movement (μm/hour)	1.0	34*	1.5***	65***	1.7**	12	1.9***	2	1.2	−11	1.1	−3	0.9	−4
Proliferation (% BrdU positive)	1.0	27*	2.2***	78***	0.6*	2	0.8	−15	0.6*	−18	0.7	−3	0.7*	20

over, proliferation rates of fibroblasts in the cell-derived 3D matrices were higher (Table 1). It is noteworthy that 3D collagen gels did not mimic the cell-derived 3D matrix in terms of rates of attachment and acquisition of elongated cell shape, migration, and proliferation (Table 1) (*18*).

Because cells within collagen gels become dependent on a particular integrin receptor (*12*), we tested the hypothesis that altered integrin usage might underlie the enhanced cell matrix–dependent biological functions in 3D matrices. Integrin usage (functional dependence) was restricted to only the $\alpha_5\beta_1$ integrin, a major fibronectin receptor. A function-blocking monoclonal antibody (mAb) specific for the α_5 integrin subunit blocked all enhanced cellular responses to 3D matrices (Fig. 2 and Table 1). Functional inhibition was less efficient on fibronectin or other substrates, where other integrins are also used. For example, α_5 mAb inhibited cell attachment to both tissue- and cell-derived 3D matrix by nearly 90% (Table 1 and Fig. 2A), yet inhibited attachment to fibronectin by only 36%. Fibronectin dependence was confirmed with antibodies to fibronectin, which inhibited attachment to cell-derived 3D matrix by 76% and to 2D fibronectin by 95% (*19*). Strong dependence on α_5 for the matrix-induced spindle-shape morphology was also observed (68% inhibition in the cell-derived 3D matrix versus 29% on fibronectin at 5 hours after plating; no cell detachment occurred). Migration in 3D matrix was also dependent on α_5 (65% inhibition versus 2% or 12% on solubilized or flattened cell-derived matrix, respectively). Enhancement of cell proliferation rates also depended on α_5 integrin (78% versus 27%, Table 1).

Cells plated into tissue- or cell-derived 3D matrices showed complete triple colocalization of α_5 integrin, paxillin, and fibronectin (Fig. 3, C and F), similar to the colocalization defining 3D-matrix adhesions in vivo (compare Figs. 1H and 3A; also compare Fig. 1J to Fig. 3, C and F). The properties of 3D-matrix adhesions observed in vivo or with in vivo–like 3D matrix environments could be due either to the three-dimensionality of the matrix or to its composition. Because these structures were so heavily dependent on functional $\alpha_5\beta_1$ fibronectin receptors, we tested whether 3D pure fibronectin environments could generate 3D-matrix adhesions. Conversely, because these adhesions might be induced by the components of cell-derived matrices rather than by their three-dimensionality, we also tested whether an identical matrix flattened by mechanical compression to form a virtually 2D matrix could generate 3D-matrix adhesions. Neither 2D matrix nor 3D fibronectin showed the characteristic, complete triple colocalization of α_5 integrin, paxillin, and fibronectin (compare Fig. 3, C and F, to Fig. 3, D and E).

If the flexibility or deformability of 2D fibronectin substrates is suppressed by fixation and cross-linking, the formation of fibrillar adhesions is abolished and $\alpha_5\beta_1$ accumulates in large focal adhesions (*9, 20*). Similarly, rigidifying cell-derived 3D matrices abolished 3D-matrix adhesions, which were replaced by short adhesions similar to those found on fixed 2D substrates (*18*). We recently reported that the translocation of the α_5 integrin out of focal adhesions into fibrillar adhesions is not dependent on de novo protein synthesis (*9*). In the same way, 3D-matrix adhesions were formed successfully even in the presence of cycloheximide (*18*). Therefore, a pliable 3D state of the matrix and molecules besides fibronectin are required to provide a permissive substrate for organization of 3D-matrix adhesions, but new protein synthesis is not required.

Because 3D-matrix adhesions enhanced cellular functional activities compared to 2D adhesions, we further compared their molecular compositions. Human fibroblasts were plated on 3D matrices and alternative substrates, and localization of various components was determined by immunofluorescence staining (*18*). These studies established that antibodies to paxillin, vinculin, FAK, phosphotyrosine, α-actinin, and activated β_1 integrin all colocalized with α_5 integrin mAb only in cells adhering to the tissue- or cell-derived 3D matrices (Table 2). In contrast, the β_3 integrin failed to colocalize (Table 2). Similar results were obtained when NIH-3T3 cells or mouse NC-15 neural crest–like cells were plated in human fibroblast-derived 3D matrices (*19*). Localization of all of these molecules to 3D-matrix adhesions was disrupted by the function-blocking α_5 integrin mAb (*18*) and by an inhibitory β_1 integrin mAb, but not by a function-blocking α_v integrin mAb (*19*). These components redistributed to small focal adhesion–like structures, apparently reverting the pattern of organization to that characteristic of 2D rigid substrates (*18*). The morphology of the 3D-matrix adhesions also differed from classical adhesions in their long and slender appearance [19 μm long with a length/breadth

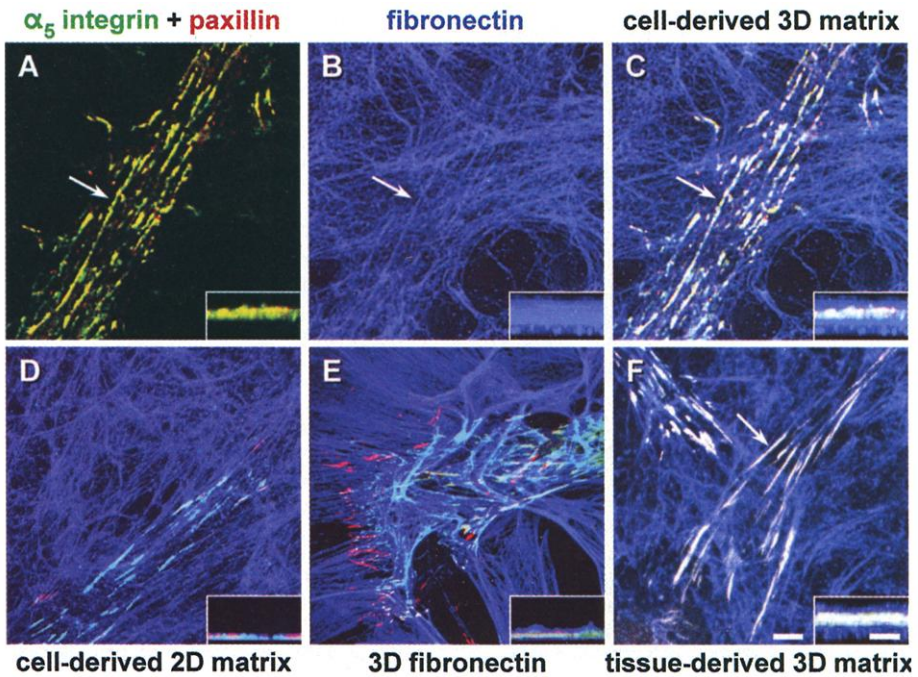

Fig. 3. Both 3D organization and cell-derived matrix components are required for formation of 3D-matrix adhesions. Human fibroblasts were cultured overnight in intact, cell-derived 3D matrix (**A** to **C**), on cell-derived matrix mechanically flattened to form a 2D matrix (**D**), in a 3D matrix composed solely of fibronectin fibrils (**E**), or in mouse tissue–derived 3D matrix (**F**). Triple-label localization of α_5 integrin (green), paxillin (red), and fibronectin [blue, (B)] was performed. The yellow (A) represents the merged labels of α_5 in green and paxillin in red. Triple-merged images for the indicated matrices are shown in (C) to (F). Note that complete triple colocalization (white) is observed only with in vivo–like, cell-derived 3D matrix (C) or mouse tissue–derived 3D matrix (F) in 3D-matrix adhesions (arrows). Moreover, on all other substrates, mainly focal adhesions (red, or purple due to merging red and blue) and fibrillar adhesions (turquoise, merged green and blue) are observed. Insets represent 90° rotated projections showing the thickness of each substrate (blue) and the position of the cell adhesion structures in relation to the substrates. For example, the inset in (C) shows intercalation of adhesive structures (white) near the center of the thick, cell-derived 3D matrix (blue). Scale bars, 5 μm.

axial ratio of 33, versus 1.5 to 3 μm long and axial ratio of 3 to 7 for focal and fibrillar adhesions; see (*18*)]. Hence, the molecular composition of the 3D-matrix adhesions differs from that of both focal and fibrillar adhesions and is critically dependent on the $\alpha_5\beta_1$ integrin.

In cells plated onto planar fibronectin, antibodies to both tyrosine-phosphorylated FAK (phospho-FAK^{397}) and paxillin (phospho-paxillin^{31}) localized to focal adhesions but not to fibrillar adhesions (e.g., Fig. 4A, e to h). This adhesion-based tyrosine-phosphorylation signaling was compared in cell-derived 3D matrix. Even though both FAK and paxillin proteins were colocalized with α_5 integrin in 3D-matrix adhesions, only phospho-paxillin^{31} colocalized with α_5 integrin, whereas phospho-FAK^{397} was absent from most of the length of 3D-matrix adhesions (Fig. 4A, a to d). The absence of phosphorylation could not be attributed to lack of FAK turnover in stable adhesions, because the same pattern was

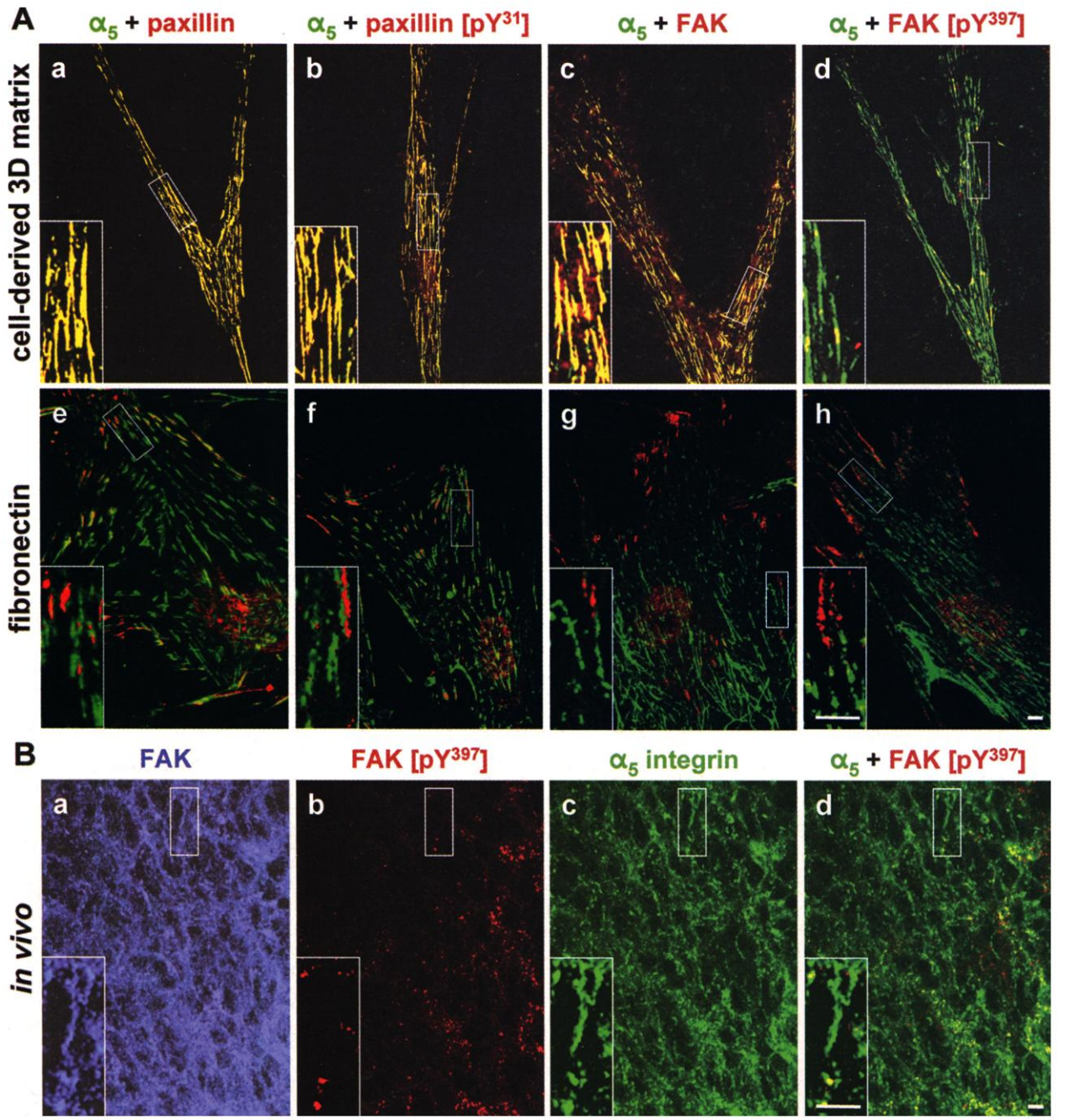

Fig. 4. 3D-matrix adhesions contain tyrosine-phosphorylated paxillin (pY^{31}), but not tyrosine-phosphorylated FAK (pY^{397}). (**A**) Fibroblasts were cultured overnight in cell-derived 3D matrices (a to d) or on fibronectin-coated cover slips (e to h). Samples were double-stained for α_5 integrin (green) and the following second molecules (red): paxillin (a and e), phospho-paxillin^{31} (b and f), FAK (c and g), or phospho-FAK^{397} (d and h). Note that even though FAK protein colocalizes with α_5 integrin in a similar manner to paxillin and phospho-paxillin^{31} in 3D matrices, phospho-FAK^{397} does not, except in small focal sites. In contrast, the molecules show minimal colocalization on fibronectin-coated surfaces. (**B**) Confocal images of indirect immunofluorescence staining of a cryostat section of an E13.5 mouse embryo, showing craniofacial mesenchymal cells. Samples were stained for FAK (a, blue), phospho-FAK^{397} (b, red), α_5 integrin (c, green), and α_5 integrin merged with phospho-FAK^{397} (d). Note that FAK protein colocalizes with α_5 integrin, but phospho-FAK^{397} appears in a punctate pattern colocalizing poorly with α_5 integrin, as in the cell-derived 3D matrix [compare (A) d to (B) d]. Insets are magnified views of the boxed areas. Scale bars, 5 μm.

Table 2. Molecular composition of cell-matrix adhesions.

Molecule	Antibody used	Focal adhesion	Fibrillar adhesion	3D-matrix adhesion
α_5 integrin	mAb11 (human), 5H10-27 (mouse)	−*	+	+
β_1 integrin	9EG7	+	+	+
β_3 integrin	VI-PL2	+	−	−
Fibronectin	R745	−*	+	+
α-actinin	BM-75.2	+	±	+
F-actin	(phalloidin)	+	+	+
Talin	4392	+	+	+
Tensin	T13820	+	+	+
Vinculin	VII F9B11	+	−	+
Phosphotyrosine	4G10	+	−	+
FAK	4.47	+	−	+
FAK^{397}	44-624	+	−	−
Paxillin	394	+	−	+
Paxillin^{31}	44-720	+	−	+

*Except at the periphery of the structure.

observed in cells plated for only 15 min and in actively migrating cells identified by time-lapse microscopy (*19*). Phospho-FAK^{397} was observed at isolated, small sites often near the ends of 3D-matrix adhesions that were also positive for β_3 integrin. Similar reductions in FAK^{397} phosphorylation were observed using three epitope-exposure staining protocols (*19, 21*). Quantitation by Western blotting confirmed decreases (by a factor of >4) in 3D versus 2D matrix without significant reductions in paxillin or ERK phosphorylation (*18*). These results indicate that adhesive interactions with 3D ECM can selectively induce paxillin phosphorylation on Tyr^{31} without concomitant colocalization of Tyr^{397}-autophosphorylated FAK. A similar discrepancy in staining for FAK protein but not phospho-FAK^{397} was confirmed for mouse mesenchymal cells in vivo (Fig. 4B). This discrepancy implies independent regulation of FAK and paxillin phosphorylation throughout most of the length of 3D-matrix adhesions, and it suggests the need for caution in applying conclusions from planar cell culture to native 3D matrix signaling functions. Because cells invading the placenta show elevated phospho-FAK (*22*), FAK may play different roles in invasion of dense tissues versus migration in 3D matrices.

We speculate that the focal and fibrillar adhesions studied in vitro represent exaggerated precursors of in vivo 3D-matrix adhesions. Focal adhesions on 2D substrates mediate firm adhesion to relatively rigid substrates (*23*), and they cooperate with fibrillar (ECM) adhesions to generate fibrils from pliable fibronectin (*9, 20*). Fibroblasts initially require culture for days at high cell density to generate 3D matrices and evolve 3D-matrix adhesions, yet when added back to cell-free 3D matrices, they begin regenerating 3D-matrix adhesions within 5 min (*18, 19*). Requirements included three-dimensionality, integrin $\alpha_5\beta_1$, fibronectin, other matrix component(s), and pliability. Taken together, our findings challenge to some extent the use of traditional tissue culture conditions for understanding the in vivo structure, functions, and signaling of cell adhesions in 3D migratory environments. They also indicate the value of substituting tissue- or fibroblast-derived 3D matrices for traditional 2D substrates in vitro. Current concepts of the biological and signaling roles of classical focal and fibrillar adhesions need to be reexamined in light of these findings on 3D-matrix adhesions.

References and Notes

1. B. M. Jockusch *et al.*, *Annu. Rev. Cell Dev. Biol.* **11**, 379 (1995).
2. K. M. Yamada, B. Geiger, *Curr. Opin. Cell Biol.* **9**, 76 (1997).
3. S. K. Sastry, K. Burridge, *Exp. Cell Res.* **261**, 25 (2000).
4. J. C. Adams, *Cell Mol. Life Sci.* **58**, 371 (2001).
5. R. O. Hynes, *Cell* **69**, 11 (1992).
6. M. A. Schwartz, M. D. Schaller, M. H. Ginsberg, *Annu. Rev. Cell Dev. Biol.* **11**, 549 (1995).
7. S. Huang, D. E. Ingber, *Nature Cell Biol.* **1**, E131 (1999).
8. E. Zamir *et al.*, *J. Cell Sci.* **112**, 1655 (1999).
9. R. Pankov *et al.*, *J. Cell Biol.* **148**, 1075 (2000).
10. C. D. Roskelley, M. J. Bissell, *Biochem. Cell Biol.* **73**, 391 (1995).
11. T. Elsdale, J. Bard, *J. Cell Biol.* **54**, 626 (1972).
12. P. Friedl, E. B. Brocker, *Cell. Mol. Life Sci.* **57**, 41 (2000).
13. J. T. Parsons, K. H. Martin, J. K. Slack, J. M. Taylor, S. A. Weed, *Oncogene* **19**, 5606 (2000).
14. C. E. Turner, *Int. J. Biochem. Cell Biol.* **30**, 955 (1998).
15. Cells were cultured in Dulbecco's modified Eagle's medium (Life Technologies) supplemented with 10% fetal bovine serum (Hyclone), penicillin (100 U/ml), and streptomycin (100 μg/ml). Immunofluorescence was performed as described (*24*) with minor modifications: For permeabilization, 0.5% Triton X-100 was added to the fixing solution for 5 min, and the phosphate-buffered saline washes contained 0.05% Tween 20. Cryostat sections of heads of mouse embryos (embryonic day E8.5 to E13.5), 10 μm thick, were stained after use of the M.O.M. blocking reagent (Vector Laboratories). Routine controls for staining and fluorescence channel specificity were performed. Laser scanning images (maximum projection views) were obtained with Leica and Zeiss confocal microscopes. Antibodies were obtained as described (*25*) and from Pharmingen (β_1 integrin mAb 9EG7, β_3 integrin mAb VI-PL2, and mouse α_5 integrin mAb CD49e), Transduction Laboratories (paxillin and tensin), Upstate Biotechnology (FAK), Biosource International (phospho-FAK^{397} and phospho-paxillin^{31}), Chemicon International ($\alpha_v\beta_3$ integrin LM609), and Jackson Immunoresearch (species-specific secondary antibodies).
16. Cell attachment after 10 min was determined after nuclear staining with bisenzimide H3342 fluorochrome by determining numbers of nuclei with the use of MetaMorph 4.5.3 software (Universal Imaging); the average value obtained on fibronectin was normalized to 1.0 arbitrary unit. For measurement of cell morphology, human fibroblast plasma membranes were stained in suspension with 1,1′-dioctadecyl-3,3,3′,3′-tetramethylindocarbocyanine perchlorate (DiI; 4 μg/ml) and cultured, and the elliptical form factor (EFF = length/breadth) was digitally determined using MetaMorph 4.5.3. Cell migration was measured as described (*26*). For measurement of proliferation, fibroblasts (6×10^4 cells/ml) were cultured overnight with bromodeoxyuridine (BrdU; 27 μg/ml), fixed, and double-stained with antibodies to lamin B (to determine total cell number) and to BrdU (to identify replicating cells). For morphometric comparisons of 3D and 2D adhesions, see (*18*).
17. Cover slips were coated with fibronectin, laminin-1, vitronectin, or collagen I at 5 μg/ml. Collagen gels (Collagen Biomaterials) were 1 mg/ml. Cell-free 3D matrices were prepared as described (*27*), except that 10- to 15-μm sections of mouse craniofacial tissue or heavily confluent 5-day cultures of NIH-3T3 cells were used; dextran and precoating of surfaces with gelatin were omitted from the protocol. Local regions of 3D matrices were mechanically compressed by applying a weight of 158 g to an area of 113 mm^2 for 2 min to generate a flattened "2D matrix." Alternatively, cell-derived 3D matrices were solubilized in 5 M guanidine containing 10 mM dithiothreitol and 5 mM phenylmethylsulfonyl fluoride. The dissolved matrix components ("2D mix") were coated on cover slips at concentrations of 5 to 50 μg/ml. Fibrillar fibronectin deposits were prepared as described (*28*) without the use of urea. All cover slips were blocked with 2% heat-denatured bovine serum albumin before use. Rigidified cell-derived matrices were produced by covalent fixation with 1% glutaraldehyde and blocking with 1 M ethanolamine.
18. For supplementary material, see *Science* Online (www.sciencemag.org/cgi/content/full/294/5547/1708/DC1).
19. E. Cukierman *et al.*, data not shown.
20. B. Z. Katz *et al.*, *Mol. Biol. Cell* **11**, 1047 (2000).
21. K. Hayashi *et al.*, *J. Cell Sci.* **112**, 1149 (1999).
22. D. Ilic *et al.*, *Am. J. Pathol.* **159**, 93 (2001).
23. K. Burridge, M. Chrzanowska-Wodnicka, *Annu. Rev. Cell Dev. Biol.* **12**, 463 (1996).
24. S. E. LaFlamme, L. A. Thomas, S. S. Yamada, K. M. Yamada, *J. Cell Biol.* **126**, 1287 (1994).
25. S. Miyamoto, S. K. Akiyama, K. M. Yamada, *Science* **267**, 883 (1995).
26. J. Gu *et al.*, *J. Cell Biol.* **146**, 389 (1999).
27. I. Vlodavsky, *Curr. Protocols Cell Biol.* **1**, 10.4.1 (1999).
28. D. C. Turner, J. Lawton, P. Dollenmeier, R. Ehrismann, M. Chiquet, *Dev. Biol.* **95**, 497 (1983).

29. We thank H. Imai for help with in vivo studies, C. Galbraith for suggestions, K. Clark and M. Hoffman for comments, K. Matsumoto and S. Hahn for technical assistance, and H. Grant for proofreading.

27 July 2001; accepted 25 September 2001